

INMM & ASARDA Joint Annual Meeting
May 22-26, 2023, Vienna, Austria

Deployment and Demonstration of Process Monitoring Equipment and Techniques in a Pyroprocessing Facility

Ammon Williams¹, Robert Hoover¹, Nathan Hoyt², Philip Lafreniere³, Tim Malewitz¹, and Steve Warrmann¹

1: Idaho National Laboratory, Idaho Falls, ID 83415.

2: Argonne National Laboratory, 9700 S Cass Ave, Lemont, IL 60439

3: Los Alamos National Laboratory, P.O. Box 1663, Los Alamos, NM 87545

Abstract

Significant effort has been made in the US and internationally to advance pyroprocessing as a viable used nuclear fuel reprocessing technology. While major advancements in the technology have been made, safeguards approaches are still being developed and explored. A major program exploring safeguards in pyroprocessing systems is the Material Protection, Accounting, and Controls Technologies (MPACT) program in the DOE Office of Nuclear Energy. These technologies include instrumentation such as voltammetry sensors, bubblers, thermocouples, and advanced analysis methods to provide process monitoring (PM) and nuclear material accountancy (NMA) within process equipment such as an electrorefiner. In 2022, a measurement campaign was conducted in which MPACT-developed technologies were deployed at the Idaho National laboratory (INL) within an electrorefiner located within the hotcell of the Hot Fuel Examination Facility (HFEF). Specific instrumentation utilized during the test include a voltammetry sensor developed at Argonne National Laboratory and a bubbler developed at INL. Additionally, process signatures from the electrorefiner were analyzed by researchers from Los Alamos National Laboratory to draw useful PM/NMA correlations within the data.

1 Introduction

Pyroprocessing technology to treat and recycle used nuclear fuel has been under development in the US and worldwide for many years. The MPACT program has been at the forefront of technology development for sensors, methodologies, and models that can be utilized to safeguard nuclear materials utilized in potential pyroprocessing technologies under consideration. A simplified pyroprocessing approach is shown in **Figure 1**. In this process, a used oxide fuel is mechanically declad and the oxide fuel is placed into a cathode basket within the Oxide Reduction (OR) furnace where it is reduced to metallic form. The reduced material is then removed from the OR and the residual salt is removed via a distillation process. Following salt removal, the basket with the metal material is placed into an electrorefiner (ER) as an anode, where the useful uranium (U) material is removed from the anode and deposited on a cathode where it is scraped off resulting in a U product. Over time, transuranic (TRU) chlorides accumulate in the salt which can be co-extracted along with uranium in a U/TRU recovery process. A few important safeguards locations and technologies have been highlighted in the figure.

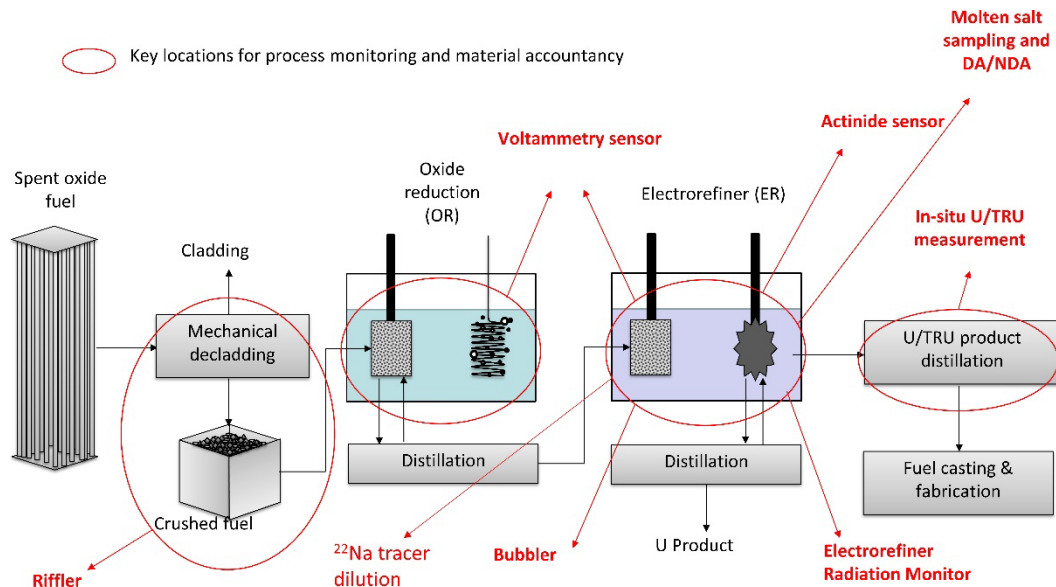


Figure 1. Schematic of a simple Pyroprocessing approach with safeguards measurement locations and technologies under investigation.

In 2020, a special issue in the *Journal of Nuclear Materials Management* [1] highlighted many of the technologies shown in the figure that are being developed under the MPACT program. Specific technologies highlighted in the issue were the OR voltammety sensor [2], triple bubbler sensor [2], the ER voltammety sensor [3], the ER actinide sensor [2], and the in-situ U/TRU measurements approach [2]. Additionally, another paper in the issue focused on integrating different safeguards measurements to further improve confidence in the measurements and the overall process [4]. An MPACT funded project not included in the special issue is a ^{22}Na radioactive tracer dilution approach to determine the total salt mass in the ER [5]. Technologies such as the riffler and ER radiation monitor were not discussed in the special issue and manuscripts for these technologies are under development and will be published later.

In 2022, a special measurement campaign was conducted under the MPACT program within a kilogram-scale ER in HFEF at INL known as the Scalable Pyrochemical Recycling testbed (SPYRE) ER to further test the developed technologies as well as to test the integration of the different signals from the sensors. The focus of this present work is to describe triple bubbler and ER voltammety results where available, and the integration of the ER sensors (process temperatures, voltages, currents, and scraper force & position).

2 Materials & Methods

The SPYRE ER is a kilogram-scale electrorefiner in the HFEF argon hotcell used for pyroprocessing research and development with irradiated nuclear fuel. As a testbed for process monitoring equipment and techniques two ER batches were conducted, the first contained U metal collected from previous used nuclear fuel ER runs and the second contained a combination of previous ER U and U/TRU products.

Triple Bubbler

The triple bubbler sensor utilized in this work was very similar to other iterations used in previous MPACT work [6-8]. Notable differences between previous bubbler designs are the dip-tube material, dip-tube inside diameters, and the incorporation of a removable steel shroud (rather than integrated). Photos of the triple bubbler design are shown in **Figure 2**. The dip-tubes were constructed of 0.25 inch (6.35 mm) outside diameter with 0.18 inch (4.57 mm) inside diameter tantalum metal tubes. The dip-tube tips had been bored to 0.1869 inch (4.747 mm), 0.1256 (3.190 mm), and 0.1870 inch (4.750 mm), for tubes 1 (long), 2 (long), and 3 (short), respectively. These dip-tubes were linked together using stainless-steel spacers which were all connected at the top while only tube 2 (middle) was connected at the base. This allowed tube 1 and 3 to float if thermal expansion was different between tubes. Finally, the dip tube assembly slid inside the shroud which provided structural support to the dip-tubes. The length of the dip-tubes were such that the tips of the longer tubes were ~1 cm from the bottom of the ER vessel with ~10 cm between the longer tubes and the shorter tube.

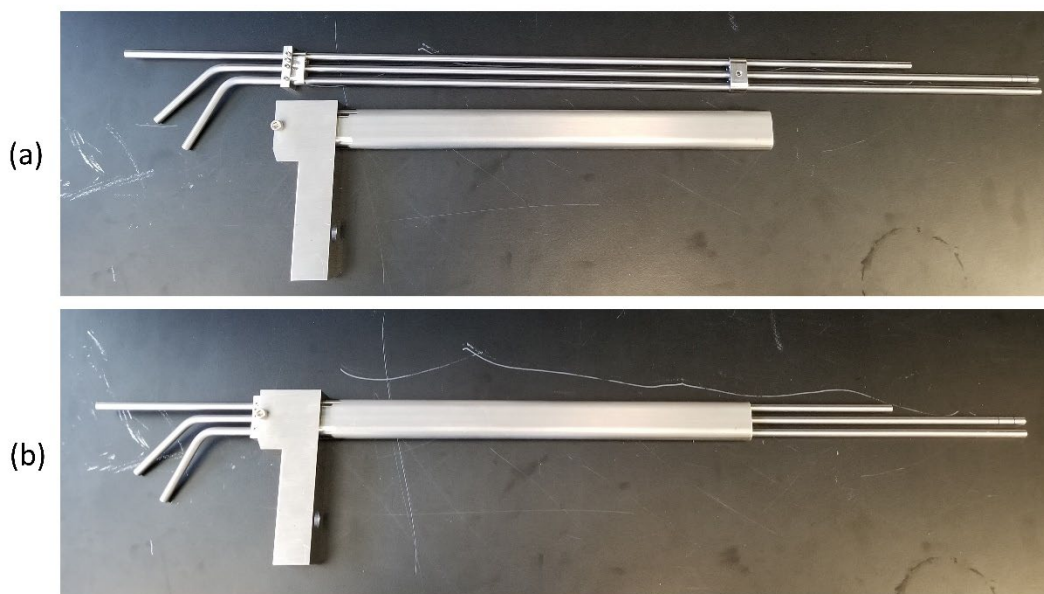


Figure 2. Photos of the triple bubbler sensor. (a) dip-tubes removed from the shroud and (b) with the dip-tubes installed.

In HFEF, the triple bubbler was installed into the ER through a mating port in the headplate. A gas instrument panel outside of the hotcell was utilized to meter gas to the dip-tubes and measure the bubble pressures. Descriptions of the panel can be found elsewhere [2]. In these experiments the gas flow was controlled between 1 and 6 standard cubic centimeters per minute (SCCM).

ER Voltammetry Sensor

Electroanalytical monitoring of the salt composition, redox state, and salt level was provided by the multielectrode array voltammetry sensor [9] shown in **Figure 3**. The sensor consisted of four working electrodes that were immersed into the salt. Signals were applied to these electrodes in a prescribed sequence that typically consisted of multiple steps including linear sweep voltammograms and electrical impedance spectroscopy. The salt level and the current densities

needed for use in electroanalytical formulas were extracted by analyzing measurements taken across the four electrodes, each of which have prescribed length differences. More details about the data analysis approach are included in Hoyt, et al. [10].



Figure 3. Multielectrode array voltammetry sensor

Process Monitoring Models

In addition to specific sensor technologies, process signals such as operating temperature, potential, and scraper position and force can be applied for the purpose of process monitoring. Techniques utilizing multi-variate approaches have been applied to process monitoring of chemical operations to ensure that they are operating in a “normal” in-control condition [11-12]. These same principles can be applied to process monitoring of the ER to ensure it is operating in an “normal” or declared mode of operation. One statistical method that is routinely used for this purpose is Principal Component Analysis (PCA) and this was applied to the ER operations of this experiment. PCA transforms the variables into a lower dimensional space where the majority of the variance is explained by a smaller set of principal components and on this space statistical tests can be performed to determine departure from normal operations.

To perform PCA, first a set of historical data X is used to train the PCA model. This data fits what would be described as normal operation. X is a matrix consisting of n rows of time series data and m columns of measurement variables. The covariance matrix C is then calculated for X . An Eigenvector decomposition calculation is performed on C as seen in equation 1.

$$C = V\Lambda V^T$$

The loading vector V of size (mxm) is reduced to only the needed number of principal components in new loading vector P of size (mxa) where the number of needed principle components a is determined by performing parallel analysis on data set X . A score matrix T is then determined by the multiplication of X and P and this score matrix is reprojected onto X as \hat{X} by multiplying T with P^T .

Subsequent signals can be tested against this modeled data in the principal component space to determine if it departs from normal operations. This is performed using a T^2 statistic calculated from a measurement vector x using equation 2.

$$T^2 = x^T V(\Lambda)^{-1} V^T x$$

If the T^2 exceeds a set threshold we are led to conclude the operation as being off normal.

3 Results and Discussions

Triple Bubbler

In preparation to start batch 1 in the ER, the new triple bubbler assembly was transferred into the hotcell and installed into the ER. Unfortunately, the existing gas lines in HFEF for the bubbler had been compromised and several days passed where the bubbler was in the salt but not bubbling. During this time, salt sat inside the dip-tubes since gas flow to push it out was unavailable. When new gas lines were finally in place, attempts to push the salt out by heating the ER headspace and purging the dip-tubes with gas was only partially successful and some residual salt remained on the walls of the tubes. As a result, the dip-tubes showed varying degrees of salt droplet interaction within the tubing (unusually high pressures and build and purge cycles). The measured pressures from the three dip-tubes are shown in **Figure 4** for the first 16 days of operation. Initially, dip-tube 1 and 3 were behaving mostly normally while dip-tube 2 showed irregular behavior. As a result, the bulk of the analysis was done excluding dip-tube 2.

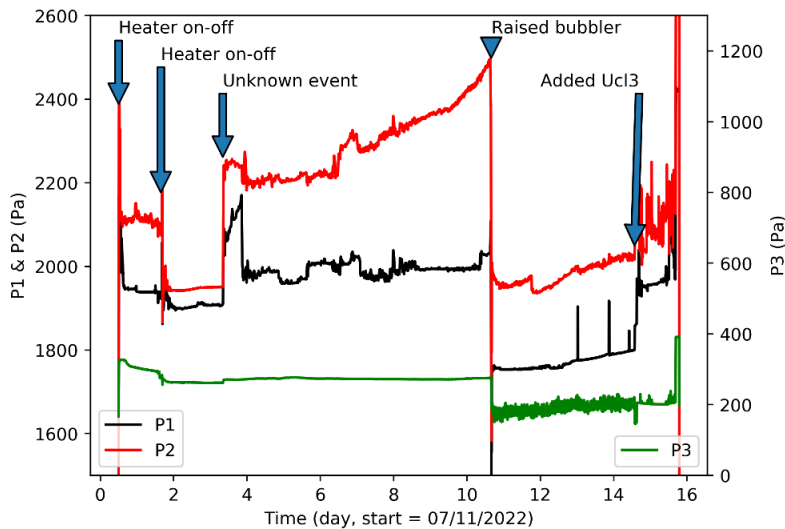


Figure 4. Dip-tube pressure measurements from the triple bubbler in the ER salt.

Events from the ER log are shown on **Figure 4** and **Figure 5**. The first two events coincide to turning the upper heaters on and then off which resulted in spikes in the salt temperature and changes in the salt density (see **Figure 5a**). The third event in the plots is not on the ER logs and is labelled as unknown. All three dip-tubes responded to the unknown event but dip-tubes 1 and 2 responded disproportionately and dip-tube 1 remained irregular thereafter. The unknown event does not appear in any of the other data streams such as temperature and it is likely that this corresponds to vibration from other activities in cell (another indication that salt droplets are interacting inside the dip-tubes). Finally, when the triple bubbler sensor was raised 0.5 inches (12.5 mm) in event 4, all three dip-tubes became irregular and for time periods beyond 16 days the magnitudes of the pressures were only qualitative. As a result, the UCl_3 addition was the only event recorded by the triple bubbler during the measurement campaign.

Figure 5a shows a plot of the salt density (from dip-tube 1 and 3). The first 3.5 days are a good representation of the salt density in the ER, including density changes as the salt temperature

fluctuated. However, beyond 3.5 days, dip-tube 1 was irregular and the density calculations have large uncertainties. Similarly, in **Figure 5b**, the depth initially corresponded closely with the ~12 cm depth measurement taken independently using a cold dip rod, all the way up until the bubbler was raised 0.5 inches (12.5 mm). The independent depth measurement measures total depth whereas the bubbler is only measuring the dip-tube submersion depth. Since the dip-tubes were approximately 1 cm from the bottom of the vessel, the total salt depth from the bubbler was ~12 cm which matched the independent measurement.

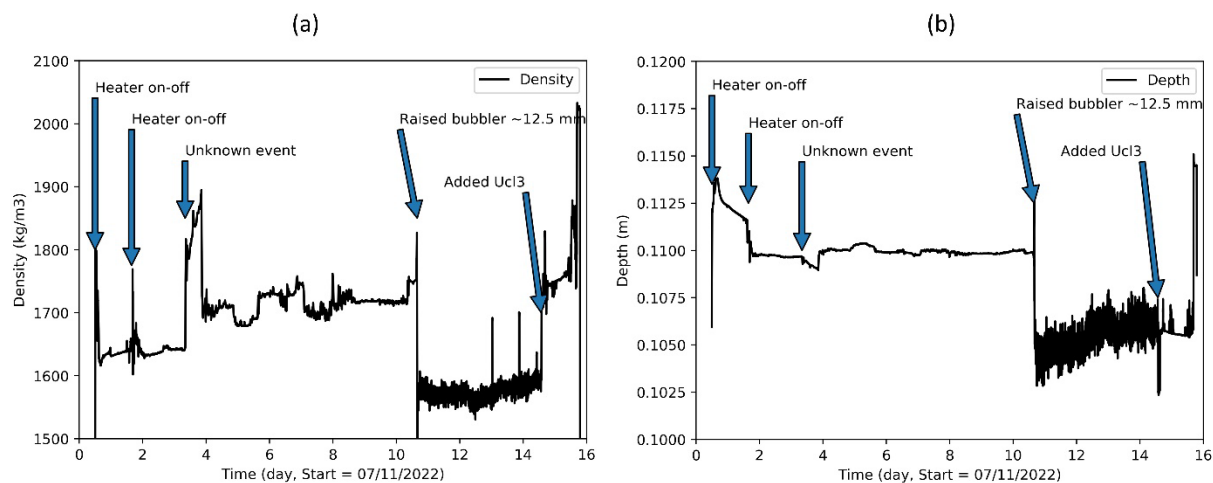


Figure 5. (a) Salt density calculated from dip-tubes 1 and 3. (b) Depth calculated from dip-tube 3 and the calculated density.

ER Voltammetry

Argonne's voltammetry sensor was used to monitor the HFEF electrorefiner during the operations occurring from May through September 2022. The sensor operations were not continuous over that entire period, but instead lasted for a total of 688 hours (29 days) during occasions when key electrorefiner activities were taking place. In total, 8,589 concentration measurements were taken over this period.

The sensor was able to monitor a wide range of activities during this time including basket insertions, salt additions, electrorefining, and vessel cleanup. Linear sweep voltammetry (LSV) traces from mid-September are shown in **Figure 6**. The fidelity of the peaks and their correct scaling with respect to electrode depth are indicative of proper operations of the sensor (Electrode 1 being the deepest, with Electrode 4 being the shallowest). Peaks associated with uranium, plutonium and lanthanide chlorides were present.

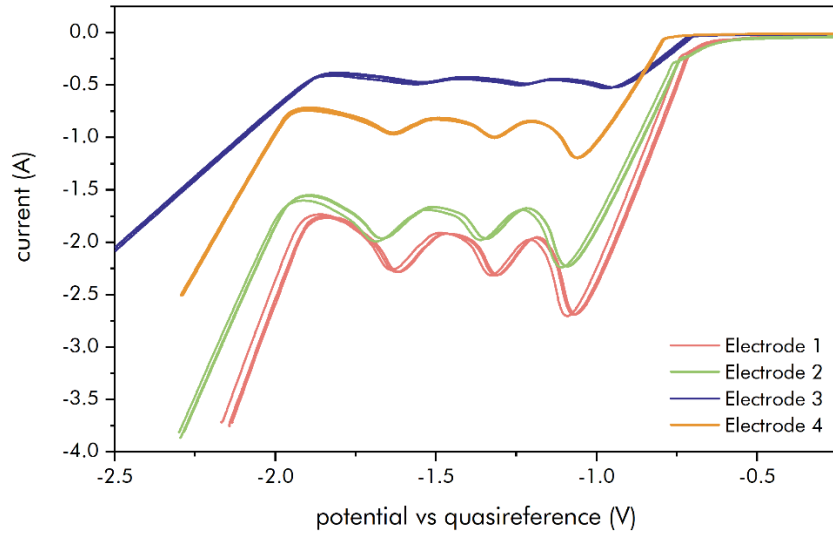


Figure 6. LSVs for all four electrodes during typical HFEF ER monitoring sequence (measurements #100, #175, and #250 are shown for a given sequence conducted across all four electrodes).

Full analysis of the data taken during this period is still pending. Representative examples of analyzed data taken earlier during a FY21 measurement campaign are shown in **Figure 7** and **Figure 8**. These figures show the sensor response during an operation where fresh LiCl-KCl salt was added to the electrorefiner vessel during the break between $t = 30$ hr and $t = 120$ hr. As shown, the sensor in this instance was clearly able to measure the height difference that resulted from the added salt, along with the decrease in uranium concentration that occurred due to dilution. Measurements during a brief temperature transient that occurred in the vessel at $t = 25$ hr are also shown. Here, a brief off-normal rise in temperature resulted in a small increase in salt height along with an associated decrease in concentration. The fact that the sensor could detect these types of minor perturbations (e.g., the ~ 1 mm salt level rise) shows its promise for detecting off-normal behavior associated with material diversions.

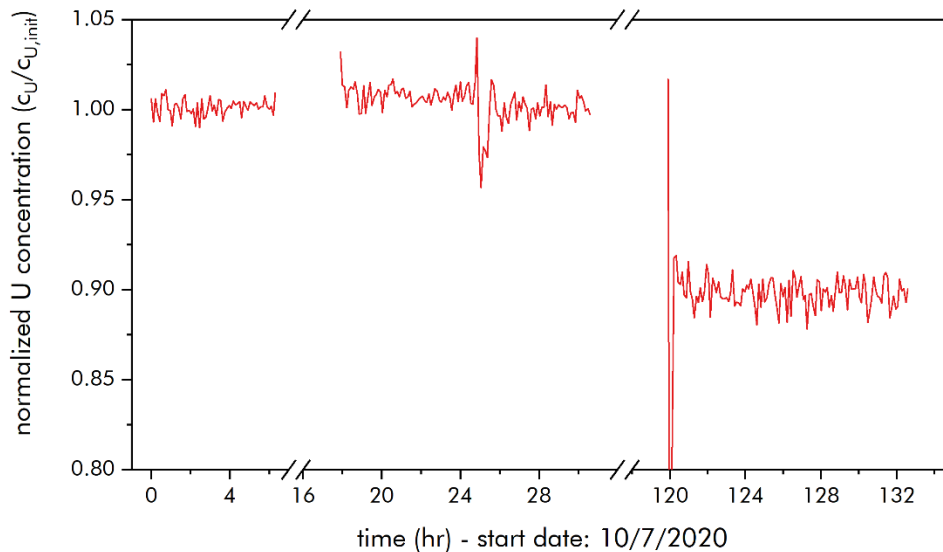


Figure 7. Normalized concentration versus time during salt addition process.

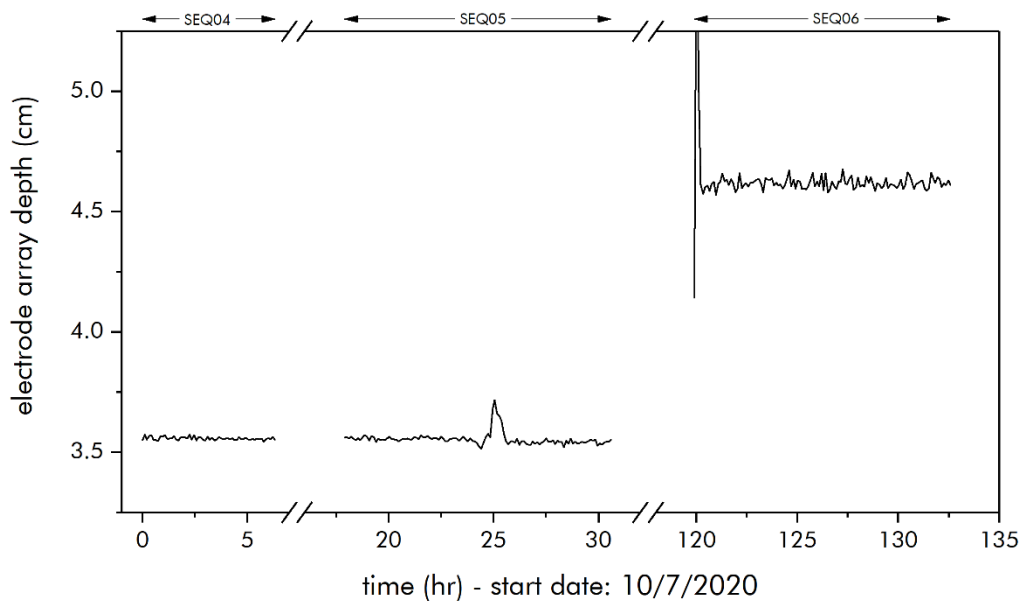


Figure 8. Salt height versus time during salt addition process.

Process Monitoring Model

The PCA approach was applied to the ER runs. The data was filtered as normal operations assuming a cell sense potential ~ 0.5 V, an operation temperature of ~ 500 °C, and the ER scraper in a retracted position. Data was filtered to include data points that included these conditions and this was utilized as the historical dataset to generate the PCA model. The entirety of the data of ER operations was transformed into vectors of observations for each time. Plots of the Scraper Position and cell potential for the entirety of the time assessed are seen in **Figure 9**. These and the other variables (Anode potential, Cathode potential, Temperature in the salt and headspace where the electrode was located, Scraper Force) were each tested as vectors for the measurement every sixty seconds to calculate the T^2 statistic using equation 2. The results of these T^2 statistics are seen in **Figure 10**.

As can be seen by the T^2 results, the PCA analysis detects 15 different events. The first thirteen can be seen to correspond to thirteen different scrapings during the course of the ER operations. The final two events are noticeable in the sensor response in the cell potential. It is because at the time of this event the ER was stopped and anode removed thus the abrupt and noticeable departure in cell potential.

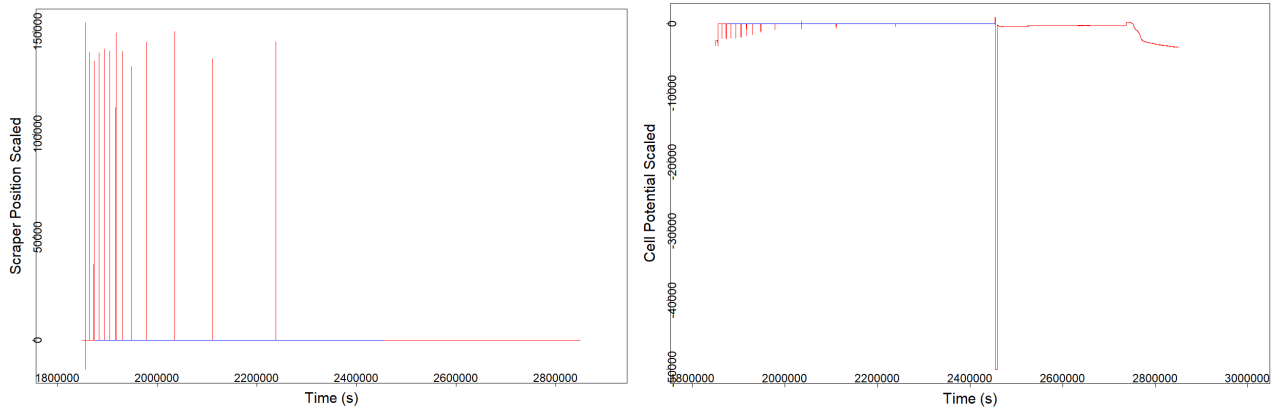


Figure 9. (a) Scraper Position Signal and (b) Cell Sense Potential Signal for ER Run starting on 7/11/2022.

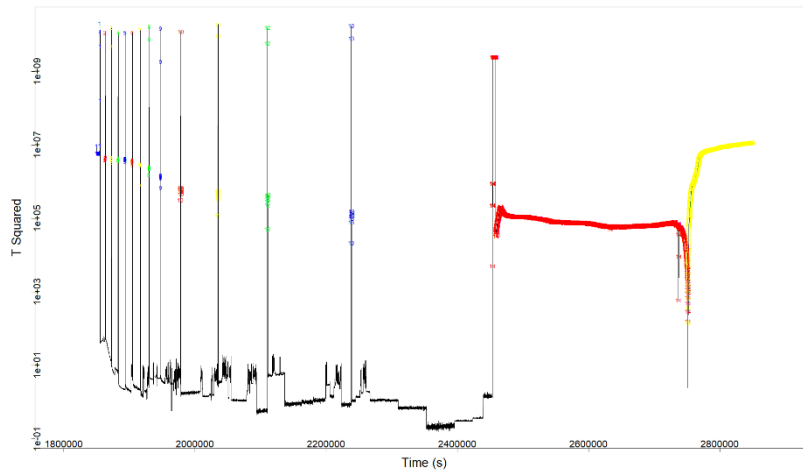


Figure 10. T2 statistic for Run Starting on 7/11/2022.

4 Summary

Two ER batches were processed through the SPYRE ER located at INL during a special measurement campaign funded by the DOE MPACT program. During these runs, process monitoring data such as the electrode voltages and currents, ER scraper position and force, salt temperatures, actinide concentrations, salt density, and salt level were recorded when possible. Results from the triple bubbler sensor were limited due to salt interactions within the dip-tubes. Preliminary data from the ER voltammetry sensor is promising and the rest of the voltammetry data is still being analyzed. Key data streams collected during the campaign were also used to develop a multivariate PCA process monitoring model. The model was successfully able to identify abnormal operating conditions such as electrode removal and scraper position faults. The destructive data analysis for samples taken during the process is pending but will be an integral part of the overall data analysis and conclusions.

5 References

1. Special Issue on the U.S. DOE MPACT Program, *Journal of Nuclear Materials Management*, Volume XLIX, No. 1, 2021.
2. A.N. Williams, G. Cao, B. Westphal, G. Galbreth, J. Sanders, J. King, D. Sell, S. Li, N. Gese, B. Serrano-Rodriguez. "Development of Safeguards Instrumentation and Technologies at the Idaho National Laboratory for an Electrochemical Facility," *Journal of Nuclear Materials Management*, Volume XLIX, No. 1, 99-115, 2021.
3. N. C. Hoyt, C. A. Launiere, E. A. Striker, "In-Process Monitoring of Molten Salt Composition by Voltammetry and Automated Sampling-Based Techniques," *Journal of Nuclear Materials Management*, Volume XLIX, No. 1, 87-98, 2021.
4. P. Lafreniere, M. Fugate, B. Key, "Advanced Integration of Safeguards Measurements," *Journal of Nuclear Materials Management*, Volume XLIX, No. 1, 66-86, 2021.
5. G. Cao, N. Larson, B. Storms, P. Kandlakunta, L. R. Cao, S. Li, "Gamma-ray spectra analysis of Molten Salts in Spent Nuclear Fuels Pyroprocessing Facilities for Mass Measurement." *Journal of Radioanalytical and Nuclear Chemistry*, 331, 3085-3091, 2022.
6. A.N. Williams, G.G. Galbreth, and J. Sanders, "Accurate Determination of Density, Surface Tension, and Vessel Depth using a Triple Bubbler System." *Journal of Industrial and Engineering Chemistry*, 63, 149-156, 2018.
7. A.N. Williams, A. Shigrekar, G. G. Galbreth, and J. Sanders, "Application of a Triple Bubbler Sensor for Determining the Density, Surface Tension, and Depth in Molten Salts." *Journal of Nuclear Materials Management*, XLVII, 47-52. 2019.
8. A.N. Williams, A. Shigrekar, G. G. Galbreth, and J. Sanders, "Application and Testing of a Triple Bubbler Sensor in Molten Salts." *Nuclear Engineering and Technology*, 52, 1452-1461, 2020.
9. J. Guo, N. Hoyt, M. Williamson, "Multielectrode array sensors to enable long-duration corrosion monitoring and control of concentrating solar power systems." *Journal of Electroanalytical Chemistry*, 884, 115064, 2021.
10. N. C. Hoyt, J. L. Willit, M. A. Williamson, "Communication-Quantitative Voltametric Analysis of High Concentration Actinides in Molten Salts," *Journal of the Electrochemical Society*, 164, H134, 2017.
11. T. Kourti, "Process Analysis and Abnormal Situation Detection: From Theory to Practice," *IEEE Control Systems Magazine*, 10-25, October 2002
12. E.L. Russell, L.H. Chiang, and R.D. Braatz, *Data-Driven Techniques for Fault Detection and Diagnosis in Chemical Processes*, London: Springer-Verlag London, 2000